

doi:10.1520/MPC20180147 / Vol. 8 / No. 3 / 2019 / available online at www.astm.org

Kavita Meduri,¹ Arianna Rahimian,^{1,2} Riley Ann Humbert,^{1,3} Graham O'Brien Johnson,⁴ Paul G. Tratnyek,⁴ and Jun Jiao⁵

A Comparative Study of Carbon Supports for Pd/Au Nanoparticle-Based Catalysts

Reference

K. Meduri, A. Rahimian, R. A. Humbert, G. O'Brien Johnson, P. G. Tratnyek, and J. Jiao, "A Comparative Study of Carbon Supports for Pd/Au Nanoparticle-Based Catalysts," *Materials Performance and Characterization* 8, no. 3 (2019): 479–489. https://doi.org/10.1520/MPC20180147

ABSTRACT

Carbon materials are promising supports for heterogeneous catalysis compared to oxide supports, such as titania, alumina, mesoporous silica, and hydrotalcite, because of their stability and relative chemical inertness. Additionally, the unique surface structures of carbon supports help control the growth, aggregation, and uniformity of the catalytic nanoparticles (NPs) hybridized with them. However, the effect of carbon supports on these NP catalysts is not well understood, affecting the optimization of this type of catalysts. In this study, palladium-gold (Pd/Au) carbon composites were systematically investigated, and the most favorable carbon support was identified. Carbon-supported Pd/Au NPs have often been favored for catalytic hydrodehalogenation (HDH) of volatile organic compounds. Hence, this study uses trichloroethylene (TCE) as model contaminant to investigate the effects of four types of carbon supports—granular activated carbon (GAC), carbon black, graphite, and graphite nanoplates—on the formation of catalytic Pd/Au NPs and their correlations to HDH reactions. Each support was chosen based on a desirable quality: GAC has a large surface area and substantial absorption capabilities, carbon black has a high surface-area-to-volume ratio and good chemical stability, graphite is the most stable form of carbon with a layered structure and thermal stability, and graphite nanoplates have large surface areas with structural stability. Characterizations of these Pd/Au-carbon composites show different NP sizes on each support, with GAC and carbon black generating smaller NPs. The HDH results suggest GAC, carbon black, and graphite nanoplates composites generate fast reaction rates. However, when comparing particle size and surface area, Pd/Au-GAC composites generate the fastest TCE degradation, providing a bigger boost to HDH rates than other types of carbon supports. More advantageously, GAC is widely available commercially with relatively low cost, and its high surface area is enabled by its high porosity, making GAC the preferred carbon support for Pd/Au NP catalyst mass production.

- Manuscript received September 7, 2018; accepted for publication November 6, 2018; published online May 10, 2019.
- ¹ Department of Mechanical and Materials Engineering, Portland State University, 1930 SW 4th Ave., Portland, OR 97201, ¹⁰ https://orcid.org/0000-0002-0950-7962 (K.M.)
- ² Emory University, 201 Dowman Dr., Atlanta, GA 30322
- Oregon State University, 105 SW 26th St. #116, Corvallis, OR 97331
- School of Public Health, Oregon Health and Science University, 3181 SW Sam Jackson Park Rd., Portland, OR 97239
- Department of Physics,
 Department of Mechanical and
 Materials Engineering, Portland
 State University, 1930 SW 4th
 Ave., Portland, OR 97201
 (Corresponding author), e-mail:
 jiaoj@pdx.edu

Keywords

palladium-gold nanoparticles, catalysts, carbon support, palladium-gold-carbon composites, granular activated carbon, graphite, carbon black, hydrodehalogenation, trichloroethylene

Introduction

Carbon is commonly chosen as a support for catalysts of chemical reactions because of its large specific surface area, high porosity, excellent electron conductivity, and relative chemical inertness. As a support for nanoparticles (NPs), it has been found to have better hydrothermal stability for heterogeneous catalysis when compared with oxide supports like titania, alumina, mesoporous silica (SiO₂), and hydrotalcite.^{1–3} Additionally, most carbon supports can be easily hybridized with metallic NPs to improve catalytic activity. Some examples include manganese oxide NPs on carbon for the oxygen reduction reaction,⁴ nickel NPs on carbon for reduction of carboxylic acids,⁵ gold-platinum NPs on carbon for methanol oxidation,⁶ and palladium-gold (Pd/Au) NPs on carbon for the hydrodehalogenation (HDH) of trichloroethene (TCE). It has also previously been shown that graphene has synergistic effects on the catalytic performance of Pd/Au NPs and improves the catalytic ability of palladium NPs.⁷ However, a comprehensive study among various carbon supports in relation to the effectiveness of their supported NP catalysts is missing. Therefore, this study focuses on the role of various carbon supports on the Pd/Au catalysts for removing TCE from contaminated water.

Palladium and gold have advantages over other metals for HDH, because palladium has been shown to be more active, stable, and selective at removing TCE than metals like platinum, zinc, and copper, and gold has been shown to act as an excellent promoter of palladium by increasing its catalytic ability. In our previous study, a simple, green process has been described to synthesize Pd/Au NPs on granular activated carbon (GAC) and graphene. This process occurs at room temperature, does not need any surfactants or stabilizers, and does not introduce any chemicals outside of the organometallic precursors and solvent. This process is both environmentally friendly and produces materials with negligible contaminations, which is ideal for characterization and testing. These catalysts are highly potent, especially against TCE.

Of the various carbon types available, the focus of this report is on four types of supports: GAC, carbon black, graphite, and graphite nanoplates. A systematic study has been carried out comparing each of these carbon forms to find the most optimum support to enhance the HDH capabilities of Pd/Au NPs. The choice of these four carbon supports is due to their individual properties and advantages.

GAC has a highly heterogeneous structure from the highly disordered nature of the active carbon structure, which consists of defective carbon layer planes in the form of twisted lamellae cross-linked by an extended carbon network. GAC is a popular choice as a catalytic support because of its inherent high adsorption, large surface area, and highly developed porosity. In the past, GAC has been used to support catalytic platinum NPs, palladium NPs, and Pd/Au NPs. In the past, GAC has been used to support catalytic platinum NPs, palladium NPs, and Pd/Au NPs. In the past, GAC has been used to support catalytic platinum NPs, and Pd/Au NPs. In the past, GAC has been used to support catalytic platinum NPs, and Pd/Au NPs. In the past, GAC has been used to support catalytic platinum NPs, and Pd/Au NPs. In the past, GAC has been used to support catalytic platinum NPs, and Pd/Au NPs. In the past, GAC has been used to support catalytic platinum NPs, and Pd/Au NPs. In the past, GAC has been used to support catalytic platinum NPs, and Pd/Au NPs. In the past, GAC has been used to support catalytic platinum NPs, and Pd/Au NPs. In the past, GAC has been used to support catalytic platinum NPs, and Pd/Au NPs. In the past, GAC has been used to support catalytic platinum NPs, and Pd/Au NPs. In the past, GAC has been used to support catalytic platinum NPs, and Pd/Au NPs. In the past, GAC has been used to support catalytic platinum NPs, and Pd/Au NPs. In the past, GAC has been used to support catalytic platinum NPs, and Pd/Au NPs. In the past, GAC has been used to support catalytic platinum NPs, and Pd/Au NPs. In the past, GAC has been used to support catalytic platinum NPs, and Pd/Au NPs. In the past, GAC has been used to support catalytic platinum NPs, and Pd/Au NPs. In the past, GAC has been used to support catalytic platinum NPs, and Pd/Au NPs. In the past, GAC has been used to support catalytic platinum NPs, and the past, GAC has been used to support catalytic platinum NPs, and the past, GAC has been used to support catalytic pl

Carbon black has a polycrystalline, three-dimensional graphite structure in which the basal planes are oriented parallel to the surface. This gives carbon black particles a relatively large surface area, which, in addition to their wide commercial availability and good chemical stability, has them excellent supports for NPs. In the past, carbon black has been used to support catalytic silver NPs. and platinum NPs.

Graphite is the most stable allotropic form of carbon, with a layered, planar structure. It has been extensively studied as supports for palldium, ¹⁷ gold, ^{18,19} and other metal NPs^{20,21} because of its stability. However, graphite has surface areas much lower than GAC and carbon black. In this study, we also use the graphite nanoplates to improve the surface areas.

The term "graphite nanoplates" refers to graphite with a thickness less than 100 nm, following the definition previously outlined.²² These nanoplates are cost-effective and possess high aspect ratios, good mechanical performance, and excellent electrical and thermal conductivity.²³ Moreover, these graphite nanoplates offer larger surface area with properties similar to those of exfoliated graphene, while retaining the structural integrity of graphite. Graphite nanoplates have been used to support catalytic platinum in a previous report.²⁴ In this study,

graphite nanoplates have been fabricated, while the GAC, carbon black, and graphite were used as-purchased to make Pd/Au-carbon composites.

Herein, "composite" refers to the material formed when the Pd/Au NPs form on the carbon supports. That is, "Pd/Au-GAC composite" refers to Pd/Au NPs on GAC support, "Pd/Au-carbon black composite" refers to Pd/Au NPs on carbon black support, "Pd/Au-graphite composite" refers to Pd/Au NPs on graphite support, and "Pd/Au-graphite nanoplate composite" refers to Pd/Au NPs on graphite nanoplate support. When referring to all these materials, the generic term "Pd/Au-carbon composite" has been used. These Pd/Au-carbon composites have been methodically characterized and tested to find the optimal carbon support for catalytic Pd/Au NPs.

Materials and Methods

CARBON SUPPORTS

The GAC used in this study (Sigma Aldrich, Catalog #242268) was crushed using a mortar and pestle and passed through a 70-µm mesh strainer for consistency with previous studies. The carbon black (Fuel Cell Store, Item #590106) and graphite powder (Aldrich, Catalog #282863) were used as-purchased. The graphite nanoplates were synthesized through a liquid exfoliation process modified from a previously established process, which involved sonicating expandable graphite (Advanced Chemicals Supplier [ACS] Material, Product #Exgraphite-170-400) in n-methyl-2-pyrrolidone (NMP) solvent with a probe sonicator in a ratio of 2:1 (volume of NMP, mL, to weight of expandable graphite, mg). After allowing the solution to settle for 45 mins, the top half was removed and centrifuged to retrieve the graphite nanoplates from the solution.

SYNTHESIS OF PD/AU NPS ON CARBON SUPPORTS

Palladium (II) acetate (98 % reagent grade, Sigma Aldrich) and tetrachloroauric (III) acid trihydrate (ACS grade, Sigma Aldrich) precursors were used to make the Pd/Au bimetallic NPs. The synthesis process uses a solution of 1.25 mg/mL of the gold precursor in acetone (ACS reagent grade), which is sonicated for 15 mins and added to a solution of 0.15 mg/mL of palladium precursor in acetone. This combined solution is sonicated for 1 h, after which it is transferred into a Teflon liner. Twenty-seven mg of the corresponding carbon support (GAC, carbon black, graphite, or graphite nanoplates) is added to this liner, and the liner is inserted into a stainless-steel autoclave. The reaction occurs for 24 h at room temperature, after which the final solution is centrifuged to retrieve the carbon-supported NPs, which are allowed to dry at room temperature.

MATERIAL CHARACTERIZATION

A Zeiss Sigma FEG VP scanning electron microscope (SEM) with energy-dispersive X-ray spectroscopy (EDS) and a FEI Tecnai F20 high-resolution transmission electron microscope (TEM) equipped with scanning transmission electron microscopy (STEM) and EDS capabilities were used for the imaging and chemical analysis of the specimens. The as-made specimens were analyzed step-by-step in the SEM and TEM to further analyze the distribution, size, shape, and morphology of the NPs on each carbon support. First, the bare carbon supports were analyzed prior to synthesis. After synthesis, each specimen was characterized in detail. Because all the specimens were made using identical methods, this allowed a direct comparison between the findings. After synthesis, the solution in which the composites were formed were also tested, and finally, each composite was tested against TCE for HDH data, as detailed in the following.

QUANTIFICATION OF NPS RETAINED BY CARBON SUPPORTS DURING SYNTHESIS

Ultraviolet-visible (UV-vis) measurements were conducted to calculate the uptake, or retention, of NPs by each support during synthesis. While a known quantity of the precursor solution was introduced, here, the actual number of NPs formed on the carbon supports has been quantified as a mass concentration. A Shimadzu UV 3600 UV-vis Spectrophotometer with a Starna 1-Q-10 Cuvette was used to collect absorbance data.

A previously published technique using Pd/Au NPs²⁹ has been adopted and modified here to calculate the amount of NPs retained by each carbon support. In brief, the reaction solutions before and after synthesis were analyzed to measure the formation and uptake of NPs on the supports. A number of calibrations were performed to determine the relative concentrations of each component (palladium precursor solutions, gold precursor solutions, bimetallic precursor solutions, palladium NP solutions, gold NP solutions, and bimetallic NP solutions). The absorbance of the reaction solution after synthesis was analyzed both before and after centrifugation. However, these values did not vary greatly (the largest difference being 0.007 arbitrary units [a.u.]), suggesting centrifugation does not significantly affect the concentration of the NPs present in these solutions. For consistency, the centrifuged values have been reported both for calibrations and retention of NP results.

CATALYTIC REACTIVITY TESTING

Each run used 20 mg of the material with 50 mg/L (or 50 ppm) of TCE (99.5 %, Aldrich, Catalog #251402) in deionized (DI) water in a batch reactor with crimp-sealed rubber septum stoppers. The vial containing the catalyst material and 120-mL DI water (with 30-mL headspace) was spiked for 20 min with 99.9 % hydrogen gas, crimp-sealed, injected with saturated TCE solution, and rotated at 50 r/min. Data were collected at fixed intervals for 60 min or until the TCE was undetectable. The reaction was monitored through headspace gas chromatography (GC) using an HP 5890 Series II GC equipped with a flame ionization detector and a DB-624 Agilent J&W column.

Results and Discussion

Carbon supports have often been used to support palladium and gold NPs, especially in the form of GAC,³⁰ carbon black,³¹ and graphite.³² These Pd/Au-carbon composites were found to be favorable catalysts for removal of TCE via HDH,⁷ synthesis of hydrogen peroxide,³⁰ electrooxidation of formic acid,³¹ etc. However, a systematic, comparative study between the different types of carbon forms as supports for these bimetal NPs is still lacking. The four supports all have beneficial properties as supports for catalysts: both GAC and carbon black have adsorptive properties, while graphite and graphite nanoplates have more stable, ordered structures. Hence, a detailed analysis is carried out to identify the most suitable support. Specifically, the shape, size, and distribution of NPs over the GAC, carbon black, graphite, and graphite nanoplates have been studied. Next, the number of NPs actually formed on the supports, or retention of the NPs by the supports, has been quantified using UV-vis measurements. Finally, these composites have been tested against TCE for HDH studies.

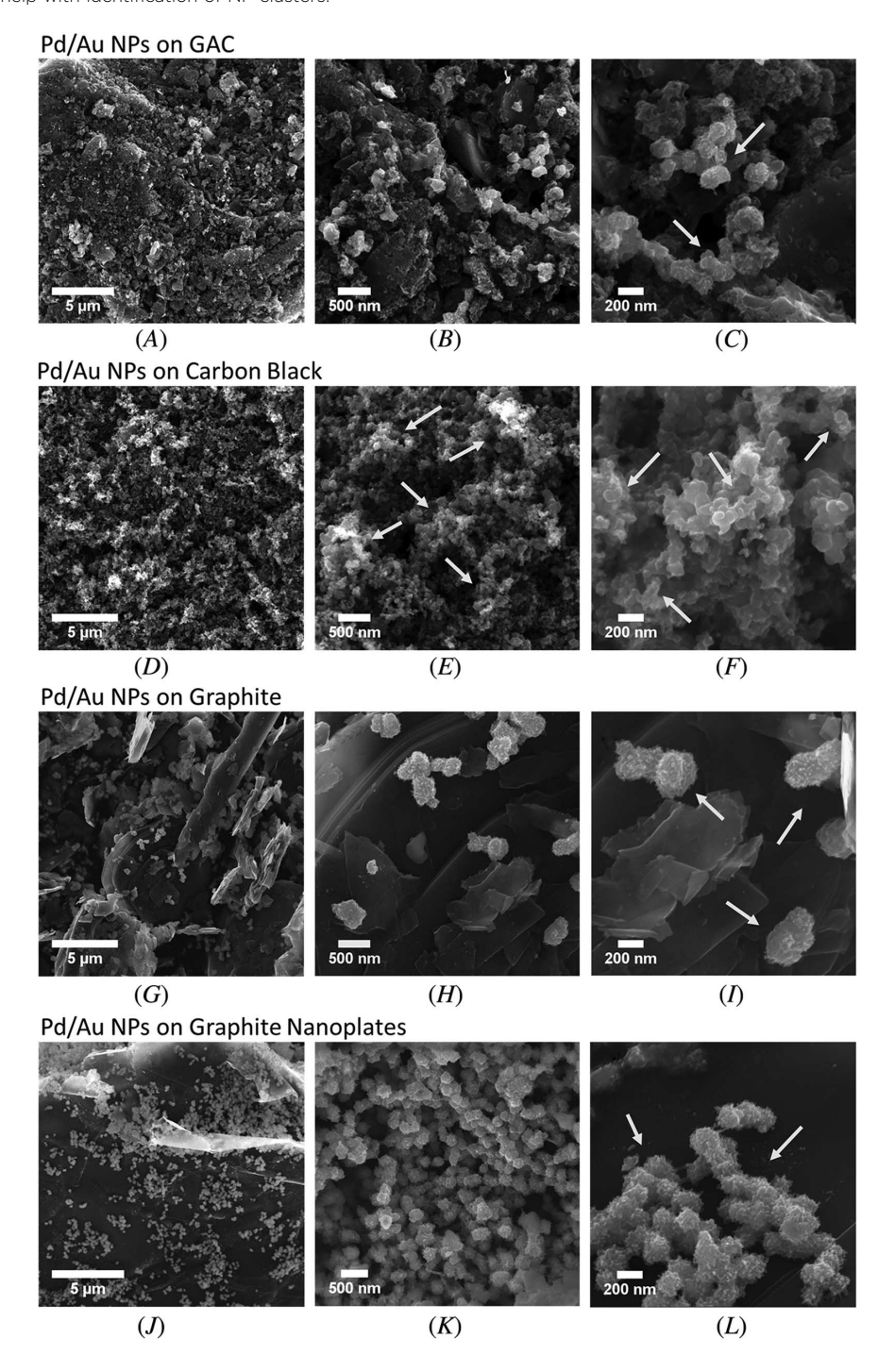
CHARACTERIZATION OF CARBON-SUPPORTED PD/AU NPS

The Pd/Au NPs were fabricated on the GAC, carbon black, graphite, and graphite nanoplate supports using identical procedures; however, a difference in the NP formation was observed on each support. All four composites have been characterized using the SEM, as seen in **figure 1**. The arrows are pointing toward some NP clusters for ease of identification.

In figure 1A-C, a Pd/Au-GAC composite specimen has been characterized, showing bimetallic NP clusters over the surface of GAC. Figure 1A shows that the NP clusters are uniformly spread over the surface of the GAC and appear to be in the same size range. The GAC surface has been further examined in figure 1B at a higher magnification, showing that the NPs appear to have an irregular morphology. At the highest magnification, seen in figure 1C, it appears that smaller NPs aggregate to form clusters. The NP clusters are further examined more specifically in later parts of the article.

The Pd/Au-carbon black composite has been studied next in figure 1D–F. Seen in figure 1D, the NP clusters are hard to identify because of the highly irregular small size of the support. At higher magnifications, seen in figure 1E, the NP clusters become slightly more apparent because of the difference in contrast, as pointed out by the arrows. In figure 1F, one such cluster is observed. This cluster appears to be similar to the clusters

FIG. 1 SEM images of Pd/Au-carbon composites. From left to right, images increase in magnification. (*A*–*C*) are images of Pd/Au-GAC composites: (*A*) dispersion; (*B*) size; (*C*) topography of NPs. (*D*–*F*) are images of Pd/Au-carbon black composites: (*D*) wider distribution of NPs; (*E*,*F*) compactness of NPs. (*G*–*H*) are images of Pd/Au-graphite composites: (*G*) poor distribution of NPs over the surface of support; (*H*,*I*) relatively larger size of NPs. (*J*–*L*) are graphite nanoplates: (*J*) large number of NPs over the surface; (*K*) size; (*L*) morphology. Arrows are provided to help with identification of NP clusters.



seen on GAC. That is, this cluster also appears to be made of smaller Pd/Au NPs; however, the size of these clusters appears to be much smaller.

Next, the Pd/Au-graphite composite is examined in figure 1*G-I*. Figure 1*G* shows that, unlike the GAC and carbon black, here, the clusters are sparsely distributed over the surface of graphite. In addition, larger clusters appear to be formed than the previous two specimens, as seen in figure 1*H*. The clusters are further examined in figure 1*I*, showing the same uneven morphology.

Finally, in **figure 1***J*–*L*, the Pd/Au-graphite nanoplates are observed. In **figure 1***J*, the clusters are well distributed over the surface of the graphite nanoplates. A closer look at **figure 1***K* shows that the NPs appear to be closer together, though of a medium size. In **figure 1***L*, the same irregular morphology of the NPs is observed.

The range and average size of the NPs are presented in Table 1. The Pd/Au-GAC composite is in the range of 100-200 nm, with an average size of 146.73 ± 35.87 nm, while the Pd/Au-carbon black is in the range of 50-150 nm with an average size of 90.078 ± 53.81 nm. The Pd/Au-graphite is in the range of 200-350 nm with an average size of 273.57 ± 50.23 nm, and the Pd/Au-graphite nanoplates are in the range of 150-250 nm clustering together with an average size of 203.37 ± 42.08 nm. These observations suggest that smaller NP and clusters are formed on GAC and carbon black, while larger-sized NPs form on graphite and graphite nanoplates.

To further examine the structure of the NP clusters, advanced SEM and TEM characterization was performed. While the size of the NP clusters was found to be different over each carbon support, the structure and configuration of the NP clusters were observed to be the same. Analysis of all four Pd/Au-carbon composites produced similar results; however, because graphite nanoplates are the most electron transparent of the four carbon supports, they are most suitable for TEM, and the Pd/Au-graphite nanoplate composite results are presented in figure 2.

The SEM images figure 2A and 2B were taken of the same location on the Pd/Au-graphite nanoplate composite by two different detectors: the secondary electron (SE) and the backscattered electron (BSE) detectors. The SE detector provides information about the topography, indicating several NPs with an irregular morphology clustered together. The BSE image provides insight into the composition of the material, indicating a heavier, dense material at the core that appears brighter than the surrounding less heavy and less dense material. The dark-field STEM image in figure 2C also confirms this compositional contrast, indicating a heavy material surrounded by a less dense material. The EDS maps in figure 2D and 2E are of elemental palladium and gold, respectively, indicating a cluster of 2–5 nm of palladium NPs surrounding a core of about 20–100 nm gold NPs. Thus, it can be concluded that these bimetallic NPs form a Pd/Au core-aggregate shell structure. These bimetallic NP structures were found to be present on all of the carbon composite materials examined in this report. The size of the individual elemental NPs remains the same on all carbon supports; however, the size of the clusters was found to vary.

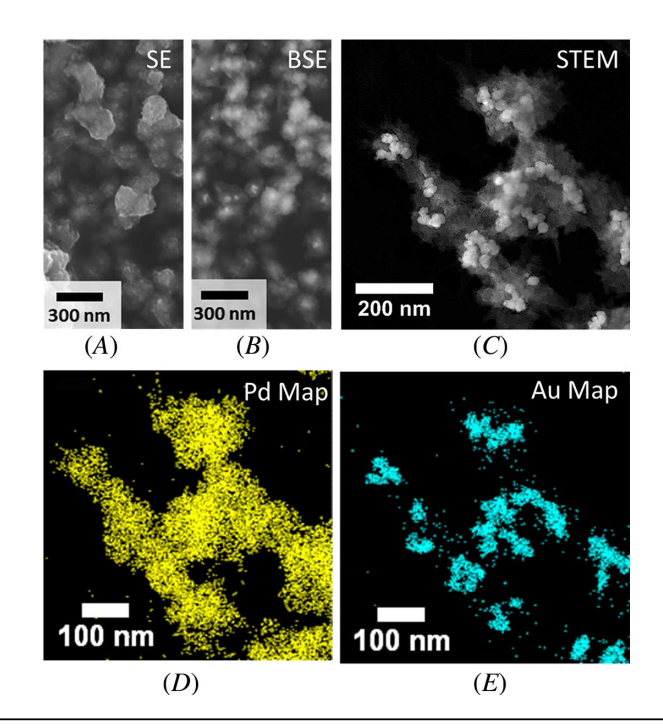
It is clear that each of the supports appears to interact differently with the metal NPs, which causes variation in sizes. One reason for this could be due to the surface of each support—both carbon black and GAC have disordered structures, while the graphite and graphite nanoplates have more ordered, layer-by-layer structures that allow the NPs to deposit at specific sites and grow uniformly. Moreover, both GAC and carbon black are highly adsorptive, which possibly disperses the metal NPs more across the surface and prevents larger aggregations from occurring. This phenomenon is presently under further investigation using more advanced techniques.

TABLE 1
Range and average size of the NP clusters for the Pd/Au-carbon composites

#	Material	Range of NP Cluster Sizes	Average Size of NP Clusters
1	Pd/Au-GAC composite	100–200 nm	146.73 ± 35.87 nm
2	Pd/Au-carbon black composite	50–150 nm	90.078 ± 53.81 nm
3	Pd/Au-graphite composite	200–350 nm	273.57 ± 50.23 nm
4	Pd/Au-graphite nanoplate composite	150–250 nm	203.37 ± 42.08 nm

FIG. 2

Electron microscopy images of Pd/Au NPs hybridized to graphite nanoplates. SEM images using (A) an SE detector and (B) a BSE detector in the same location show that the NPs are made of a core of dense material surrounded by a less dense material. The dark-field STEM image in (C) confirms this configuration. The EDS maps of (D) palladium and (E) gold indicate that the NPs are made of a gold core surrounded by a palladium shell.



RETENTION OF NPS BY CARBON SUPPORTS DURING SYNTHESIS

In order to further understand the interaction between each carbon support and the bimetal NPs, the uptake of NPs was calculated. The uptake, or retention, of the NPs by each support during synthesis has been quantified here as the mass concentration of NPs actually hybridized to each carbon support. Previously, UV-vis spectroscopy has been shown to successfully calculate the uptake of Au NPs on aluminum oxide, magnesium oxide, and SiO₂ supports.²⁹ Hence, the same method has been adopted here and modified to calculate the uptake of the NPs by the different carbon supports. The results are reported in figure 3.

Based on the calibrations and theoretical calculations, the maximum concentrations of palladium NPs and gold NPs available for uptake are 1.42 and 65.21 mg/L, respectively. All supports have an uptake of NPs of at least 88 % or more of this maximum concentration. Seen in figure 3A, GAC and carbon black have similar uptakes of palladium NPs, only leaving behind 0.07 and 0.06 mg/L, respectively. Next, graphite nanoplates appear to leave 0.1 mg/L of palladium NPs, suggesting that, despite the lack of adsorptive qualities of GAC and carbon black, the large surface area provides a platform for the NPs to deposit. Finally, graphite had the lowest uptake, leaving behind 0.16 mg/L of palladium NPs. This trend was also observed for uptake of gold NPs, seen in figure 3B, with GAC and carbon black leaving behind 3.38 and 2.86 mg/L of gold NPs, followed by graphite nanoplates leaving behind 4.51 mg/L of gold NPs and graphite with 7.34 mg/L.

While some variations in uptake in NPs were observed, the final concentrations of bimetallic NPs on the carbon supports are not significantly different. However, the sizes of the NPs and clusters on the supports are significantly different. Specifically, while graphite nanoplates have relatively similar uptake of NPs as GAC and carbon black, the NPs deposit as larger clusters on graphite nanoplates. Hence, it is believed that the extended surface area of graphite nanoplates improves the uptake of NPs and therefore the HDH removal of TCE.

HDH OF TCE BY PD/AU NPS ON DIFFERENT CARBON SUPPORTS

To understand the effect of each carbon support on the Pd/Au NPs, each specific carbon-supported catalyst was tested against model contaminant TCE. The degradation of TCE in the presence of NP catalysts with

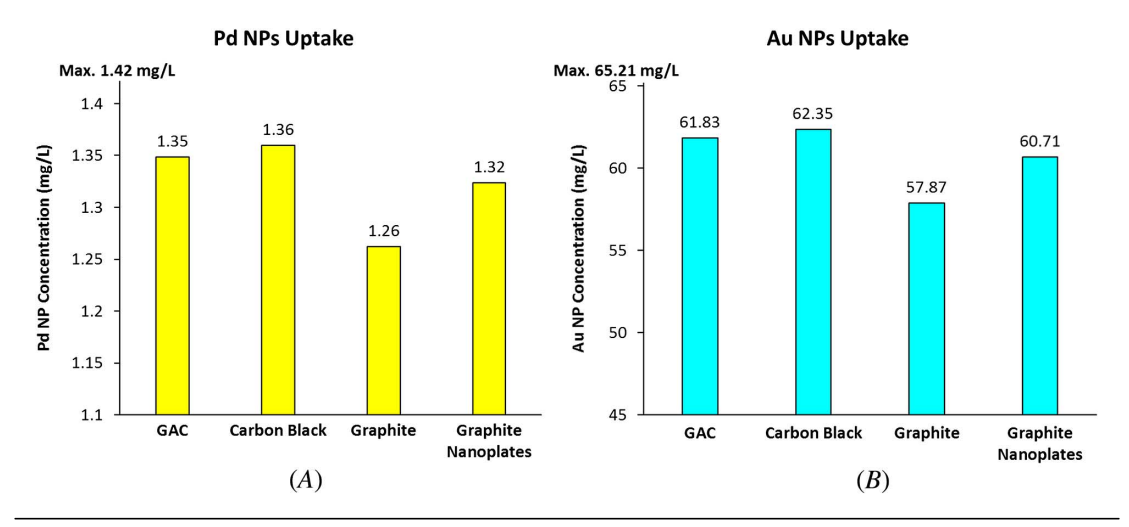


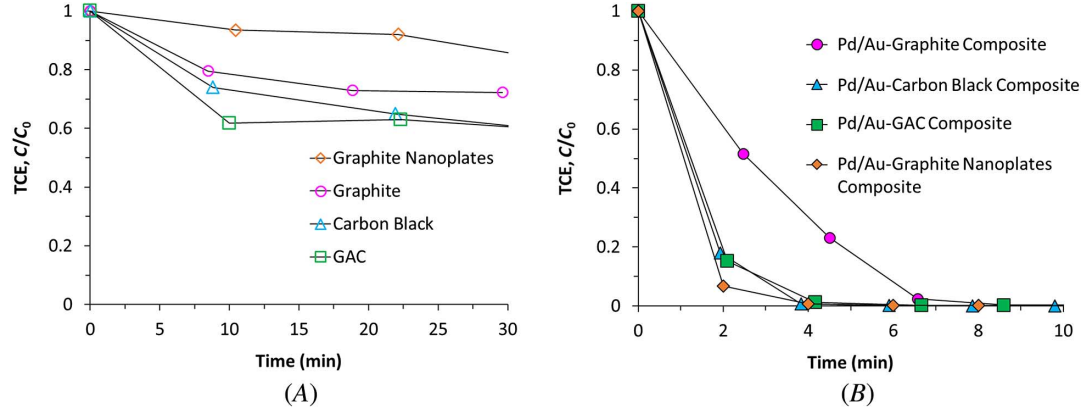
FIG. 3 Retention of (A) palladium NP and (B) gold NP on the GAC, carbon black, graphite, and graphite nanoplate supports during synthesis.

carbon supports composites was found to follow traditional HDH routes.^{7,9} This degradation of TCE is shown in **figure 4**, plotting the normalized concentration of TCE over time in the presence of the different catalysts.

As seen in **figure 4A**, first, the bare carbon materials were tested with TCE as-is. GAC appeared to have the fastest removal, adsorbing close to 40 % of TCE within the first 10 min. This was closely followed by carbon black, which also adsorbed TCE, but at a slightly slower rate, removing 30 % of TCE within the first 10 min. As expected, both the graphite nanoplates and graphite did little to remove TCE over time.

Next, Pd/Au-carbon composites were tested against TCE, as seen in figure 4B. The presence of the Pd/Au NPs caused the reactions to occur much faster. Surprisingly, the Pd/Au-graphite nanoplates composite, Pd/Au-carbon black composite, and Pd/Au-GAC composite performed roughly the same, followed by the Pd/Au-graphite composite catalyst. Multiple runs were performed, and the data were fit pseudo-first-order kinetics, following equation (1):

FIG. 4 Degradation of TCE over time, plotted as normalized concentration of TCE over time in the presence of (*A*) just carbon supports and (*B*) Pd/Au NPs hybridized to the carbon supports.



$$C = C_0 e^{-kt} \tag{1}$$

where C is the mass concentration of TCE in the bulk fluid (g_{TCE}/L) at time t (min), C_0 is the initial mass concentration of TCE in the bulk fluid (g_{TCE}/L), and k (min⁻¹) is the measured, observed (pseudo) first-order rate constant.

The Pd/Au-GAC composite specimens gave a k of 1.10 min⁻¹, while Pd/Au-carbon black composites had a k value of 1.13 min⁻¹ and Pd/Au-graphite nanoplates composites produced a k of 0.94 min⁻¹. Finally, the Pd/Au-graphite composite catalysts gave a k of 0.54 min⁻¹. This k value for the Pd/Au-GAC composites is consistent with previously observed rates.⁷

COMPARISON OF EFFICIENCY OF TCE DEGRADATIONS

It is important to note that the bare carbon supports differ from each other in surface morphology, which, in part, is responsible for the difference in the number of NPs formed on each support and the sizes of the clusters on the supports. The particle size and shape of each support is different, which has a direct impact on the catalytic HDH of TCE. A larger available surface area allows more of the TCE to interact with the catalyst and therefore HDH will occur faster. Among the four types of carbon composites of Pd/Au NPs, the Pd/Au-graphite composite has the lowest surface area among the carbon supports, and the NPs hybridized to this support grew to the largest sizes, causing an overall decrease in available surface area and, hence, interaction with the TCE. In contrast, while the NP size was relatively smaller for the Pd/Au-graphite nanoplate composites, the graphene-like properties of the large surface area of the support allow more NPs to deposit (as seen characterized previously and confirmed in the retention results). Hence, the observed k of Pd/Au-graphite nanoplates was much larger than that of the Pd/Au-graphite composite. In fact, this result is similar to previously observed data in which graphene produces the fastest rate of TCE decomposition.⁷

In the case of the Pd/Au-carbon black and Pd/Au-GAC composites, both of these carbon supports exhibit adsorption and have smaller NPs hybridized to the surfaces. This allows faster rates of degradation. Despite carbon black and GAC having different structures, ¹⁰ their adsorptive nature, combined with the dispersion and size of the metallic NPs, causes them to behave in a similar manner. However, it is also important to take particle size into consideration for available surface area of these supports. The carbon black in this study has a particle size of 50 nm for consistency with other reports, ^{14,33,34} while the GAC has a particle size closer to 70 μ m for consistency with previous reports. Hence, the carbon black used here has a much larger surface area than the GAC. Despite this, the Pd/Au-carbon black composite produces the same k as the Pd/Au-GAC composite, suggesting that when normalized for surface area, the rate of degradation of TCE for the Pd/Au-GAC composite would be much higher.

Summary and Conclusion

Four types of carbon materials—graphite, graphite nanoplates, carbon black, and GAC—have been explored for their role in supports for catalytic NPs like palladium and gold. The graphite, carbon black, and GAC were used as-purchased; however, the graphite nanoplates, which are graphite plates with thickness less than 100 nm, were synthesized using a liquid exfoliation process. The Pd/Au NPs were hybridized onto the supports using an environmentally friendly process, making Pd/Au-carbon composites. These composites were characterized using electron microscopy and spectroscopy techniques, showing different NP cluster sizes on the supports. The largest NPs were found to be on graphite and graphite nanoplate composites. Similarly, during synthesis, each carbon support was observed to hybridize, or uptake, a different number of NPs. Carbon black and GAC composites were observed to have the highest uptake, indicating that the maximum number of NPs was present on these surfaces.

The HDH results show the importance of mass transfer and surface area, indicating that the graphite nanoplate, carbon black, and GAC composites have similar rates of TCE degradation despite having varying particle sizes. The large surface area of graphite nanoplate composites allows for increased contact between the NPs and TCE. In the case of carbon black and GAC, adsorption also played a large role in the degradation of TCE. Even though these

specimens had similar rates of reaction of 1.13 and 1.10 min⁻¹ for carbon black and GAC composites, respectively, the particle sizes were vastly different. When normalized for particle size and surface area, Pd/Au-GAC composites were found to be more potent at TCE degradation than the corresponding Pd/Au-carbon black composites. The high surface area, porosity, stability, and wide commercial availability of GAC makes it the preferred carbon support, followed closely by carbon black, graphite nanoplates, and, finally, graphite. The results from this study provide insight into the role of the various carbon supports and help guide future material selection and optimization.

ACKNOWLEDGMENTS

This research is funded by the National Science Foundation (NSF) under Award Nos. 1507707 and 1508115 as well as the Oregon Nanoscience and Microtechnologies Institute. The participation of undergraduate students in this research is supported by NSF Research Experiences for Undergraduates Site Award No. 1560383. All electron microscopy and spectroscopy characterizations were completed at the Center for Electron Microscopy and Nanofabrication, located at Portland State University.

References

- 1. E. Lam and J. H. T. Luong, "Carbon Materials as Catalyst Supports and Catalysts in the Transformation of Biomass to Fuels and Chemicals," *Catalysis* 4, no. 10 (August 2014): 3393–3410, https://doi.org/10.1021/cs5008393
- H. Jüntgen, "Activated Carbon as Catalyst Support," Fuel 65, no. 10 (October 1986): 1436–1446, https://doi.org/10.1016/ 0016-2361(86)90120-1
- 3. J. Huo, R. L. Johnson, P. Duan, H. N. Pham, D. Mendivelso-Perez, E. A. Smith, A. K. Datye, K. Schmidt-Rohr, and B. H. Shanks, "Stability of Pd Nanoparticles on Carbon-Coated Supports under Hydrothermal Conditions," *Catalysis Science & Technology* 8, no. 4 (2018): 1151–1160, https://doi.org/10.1039/C7CY02098H
- 4. I. Roche, E. Chaînet, M. Chatenet, and J. Vondrák, "Carbon-Supported Manganese Oxide Nanoparticles as Electrocatalysts for the Oxygen Reduction Reaction (ORR) in Alkaline Medium: Physical Characterizations and ORR Mechanism," *Journal of Physical Chemistry C* 111, no. 3 (December 2006): 1434–1443, https://doi.org/10.1021/jp0647986
- K. Guo, Y. Zhang, Q. Shi, and Z. Yu, "The Effect of Carbon-Supported Nickel Nanoparticles in the Reduction of Carboxylic Acids for in Situ Upgrading of Heavy Crude Oil," *Energy & Fuels* 31, no. 6 (May 2017): 6045–6055, https://doi.org/10.1021/acs.energyfuels.7b00809
- 6. L. Lu, Y. Nie, Y. Wang, G. Wu, L. Li, J. Li, X. Qi, and Z. Wei, "Preparation of Highly Dispersed Carbon Supported AuPt Nanoparticles: Via a Capping Agent-Free Route for Efficient Methanol Oxidation," *Journal of Materials Chemistry A* 6, no. 1 (November 2018): 104–109, https://doi.org/10.1039/c7ta08343b
- K. Meduri, C. Stauffer, W. Qian, O. Zietz, A. Barnum, G. O'Brien Johnson, D. Fan, W. Ji, C. Zhang, P. Tratnyek, and J. Jiao, "Palladium and Gold Nanoparticles on Carbon Supports as Highly Efficient Catalysts for Effective Removal of Trichloroethylene," *Journal of Materials Research* 33, no. 16 (August 2018): 2404–2413, https://doi.org/10.1557/jmr.2018.
- 8. B. P. Chaplin, M. Reinhard, W. F. Schneider, C. Schüth, J. R. Shapley, T. J. Strathmann, and C. J. Werth, "Critical Review of Pd-Based Catalytic Treatment of Priority Contaminants in Water," *Environmental Science and Technology* 46, no. 7 (February 2012): 3655–3670, https://dx.doi.org/10.1021/es204087q
- M. O. Nutt, J. B. Hughes, and M. S. Wong, "Designing Pd-on-Au Bimetallic Nanoparticle Catalysts for Trichloroethene Hydrodechlorination," *Environmental Science and Technology* 39, no. 5 (January 2005): 1346–1353, https://doi.org/10. 1021/es048560b
- F. Rodriguez-Reinoso, J. M. Martin-Martinez, C. Prado-Burguete, and B. McEnaney, "A Standard Adsorption Isotherm for the Characterization of Activated Carbons," *Journal of Physical Chemistry* 91, no. 3 (January 1987): 515–516, https://doi.org/10.1021/j100287a006
- 11. H. X. Huang, S. X. Chen, and C. Yuan, "Platinum Nanoparticles Supported on Activated Carbon Fiber as Catalyst for Methanol Oxidation," *Journal of Power Sources* 175, no. 1 (January 2008): 166–174, https://doi.org/10.1016/j.jpowsour. 2007.08.107
- T. Gong, L. Qin, W. Zhang, H. Wan, J. Lu, and H. Feng, "Activated Carbon Supported Palladium Nanoparticle Catalysts Synthesized by Atomic Layer Deposition: Genesis and Evolution of Nanoparticles and Tuning the Particle Size," *Journal of Physical Chemistry C* 119, no. 21 (May 2015): 11544–11556, https://doi.org/10.1021/jp5130102
- 13. J. K. Edwards, S. J. Freakley, A. F. Carley, C. J. Kiely, and G. J. Hutchings, "Strategies for Designing Supported Gold-Palladium Bimetallic Catalysts for the Direct Synthesis of Hydrogen Peroxide," *Accounts of Chemical Research* 47, no. 3 (October 2013): 845–854, https://doi.org/10.1021/ar400177c
- 14. B. Fang, N. K. Chaudhari, M.-S. Kim, J. H. Kim, and J.-S. Yu, "Homogeneous Deposition of Platinum Nanoparticles on Carbon Black for Proton Exchange Membrane Fuel Cell," *Journal of the American Chemical Society* 131, no. 42 (October 2009): 15330–15338, https://doi.org/10.1021/ja905749e

- X. Xu, C. Tan, H. Liu, F. Wang, Z. Li, J. Liu, and J. Ji, "Carbon Black Supported Ultra-High Loading Silver Nanoparticle Catalyst and Its Enhanced Electrocatalytic Activity Towards Oxygen Reduction Reaction in Alkaline Medium," *Journal of Electroanalytical Chemistry* 696 (May 2013): 9–14, https://doi.org/10.1016/j.jelechem.2013.02.018
- D. Schonvogel, J. Hülstede, P. Wagner, I. Kruusenberg, K. Tammeveski, A. Dyck, C. Agert, and M. Wark, "Stability of Pt Nanoparticles on Alternative Carbon Supports for Oxygen Reduction Reaction," *Journal of the Electrochemical Society* 164, no. 9 (July 2017): F995–F1004, https://doi.org/10.1149/2.1611709jes
- 17. S. K. R. S. Sankaranarayanan, V. R. Bhethanabotla, and B. Joseph, "Molecular Dynamics Simulations of the Structural and Dynamic Properties of Graphite-Supported Bimetallic Transition Metal Clusters," *Physical Review B* 72, no. 19 (November 2005): 195405, https://doi.org/10.1103/PhysRevB.72.195405
- 18. L. J. Lewis, P. Jensen, and J.-L. Barrat, "Melting, Freezing, and Coalescence of Gold Nanoclusters," *Physical Review B* 56, no. 4 (July 1997): 2248–2257, https://doi.org/10.1103/PhysRevB.56.2248
- B. Prével, L. Bardotti, S. Fanget, A. Hannour, P. Mélinon, A. Perez, J. Gierak, G. Faini, E. Bourhis, and D. Mailly, "Gold Nanoparticle Arrays on Graphite Surfaces," *Applied Surface Science* 226, nos. 1–3 (March 2004): 173–177, https://doi.org/ 10.1016/j.apsusc.2003.11.018
- S.-P. Ping and P. B. Balbuena, "Platinum Nanoclusters on Graphite Substrates: A Molecular Dynamics Study," Molecular Physics 100, no. 13 (2009): 2165–2174, https://doi.org/10.1080/0026897021012127
- 21. S.-P. Huang, D. S. Mainardi, and P. B. Balbuena, "Structure and Dynamics of Graphite-Supported Bimetallic Nanoclusters," *Surface Science* 545, no. 3 (November 2003): 163–179, https://doi.org/10.1016/j.susc.2003.08.050
- A. Bianco, H.-M. Cheng, T. Enoki, Y. Gogotsi, R. H. Hurt, N. Koratkar, T. Kyotani, M. Monthioux, C. R. Park, J. M. D. Tascon, and J. Zhang, "All in the Graphene Family A Recommended Nomenclature for Two-Dimensional Carbon Materials," *Carbon* 65 (December 2013): 1–6, https://doi.org/10.1016/j.carbon.2013.08.038
- 23. F.-A. He, H.-J. Wu, X.-L. Yang, K.-H. Lam, J.-T. Fan, and L.-W. H. Chan, "Novel Exfoliated Graphite Nanoplates/ Syndiotactic Polystyrene Composites Prepared by Solution-Blending," *Polymer Testing* 42 (April 2015): 45–53, https://doi.org/10.1016/j.polymertesting.2015.01.002
- 24. C.-H. Hsu, H.-Y. Liao, Y.-F. Wu, and P.-L. Kuo, "Benzylamine-Assisted Noncovalent Exfoliation of Graphite-Protecting Pt Nanoparticles Applied as Catalyst for Methanol Oxidation," *Applied Materials and Interfaces* 3, no. 7 (June 2011): 2169–2172, https://dx.doi.org/10.1021/am200273s
- K. Meduri, A. Barnum, G. O'Brien Johnson, P. G. Tratnyek, and J. Jiao, "Characterization of Palladium and Gold Nanoparticles on Granular Activated Carbon as an Efficient Catalyst for Hydrodechlorination of Trichloroethylene," Microscopy and Microanalysis 22, no. S3 (July 2016): 332–333, https://doi.org/10.1017/S1431927616002518
- K. Meduri, C. Stauffer, T. Lindner, G. O'Brien Johnson, P. G. Tratnyek, and J. Jiao, "Effect of Synthesis Temperature on the Formation GAC Supported Pd and Au NPs," *Microscopy and Microanalysis* 23, no. S1 (July 2017): 1916–1917, https://doi.org/10.1017/S1431927617010248
- 27. K. Meduri, C. Stauffer, G. O'Brien Johnson, P. G. Tratnyek, and J. Jiao, "Electron Microscopy Characterization of the Synergistic Effects between Pd, Au NPs, and Their Graphene Support," *Microscopy and Microanalysis* 24, no. S1 (August 2018): 1888–1889, https://doi.org/10.1017/S1431927618009923
- 28. Y. Hernandez, V. Nicolosi, M. Lotya, F. Blighe, Z. Sun, S. De, I. T. McGovern, B. Holland, M. Byrne, Y. K. Gun'ko, J. J. Boland, P. Niraj, G. Duesberg, S. Krishnamurthy, R. Goodhue, J. Hutchison, V. Scardaci, A. C. Ferrari, and J. Coleman, "High-Yield Production of Graphene by Liquid-Phase Exfoliation of Graphite," *Nature Nanotechnology* 3, no. 9 (August 2008): 563–568, https://doi.org/10.1038/nnano.2008.215
- 29. M. O. Nutt, K. N. Heck, P. Alvarez, and M. S. Wong, "Improved Pd-on-Au Bimetallic Nanoparticle Catalysts for Aqueous-Phase Trichloroethene Hydrodechlorination," *Applied Catalysis B: Environmental* 69, nos. 1–2 (December 2006): 115–125, https://doi.org/10.1016/j.apcatb.2006.06.005
- 30. J. K. Edwards, A. Thomas, A. F. Carley, A. A. Herzing, C. J. Kiely, and G. J. Hutchings, "Au–Pd Supported Nanocrystals as Catalysts for the Direct Synthesis of Hydrogen Peroxide from H2 and O2," *Green Chemistry* 10, no. 4 (November 2007): 388–394, https://doi.org/10.1039/b714553p
- 31. R. Larsen, S. Ha, J. Zakzeski, and R. I. Masel, "Unusually Active Palladium-Based Catalysts for the Electrooxidation of Formic Acid," *Journal of Power Sources* 157, no. 1 (June 2006): 78–84, https://doi.org/10.1016/j.jpowsour.2005.07.066
- L. Gorton and T. Svensson, "An Investigation of the Influences of the Background Material and Layer Thickness of Sputtered Palladium/Gold on Carbon Electrodes for the Amperometric Determination of Hydrogen Peroxide," Journal of Molecular Catalysis 38, nos. 1–2 (November 1986): 49–60, https://doi.org/10.1016/0304-5102(86)87048-1
- 33. A. Eshghi and M. Kheirmand, "Palladium Nanoparticles Supported on Carbon Black Powder as an Effective Anodic Catalyst for Application in a Direct Glucose Alkaline Fuel Cell," *Iranian Journal of Hydrogen & Fuel Cell* 3, no. 1 (2016): 11–17, https://doi.org/10.22104/ijhfc.2016.319
- M. Bron, "Carbon Black Supported Gold Nanoparticles for Oxygen Electroreduction in Acidic Electrolyte Solution," *Journal of Electroanalytical Chemistry* 624, nos. 1–2 (December 2008): 64–68, https://doi.org/10.1016/j.jelechem.2008. 07.026